Journal of Food Engineering 247 (2019) 80–94

Contents lists available at ScienceDirect

Journal of Food Engineering

journal homepage: www.elsevier.com/locate/jfoodeng

Design and characterization of mangiferin nanoparticles for oral delivery

Rohini Samadarsi, Debjani Dutta*

Department of Biotechnology, National Institute of Technology Durgapur, Mahatma Gandhi Avenue, Durgapur, 713209, West Bengal, India

ARTICLE INFO

Keywords:
Mangiferin
β-Lactoglobulin
Antioxidant-activity
Microbial toxicity

ABSTRACT

Mangiferin, a bioactive compound with numerous therapeutic properties was extracted from *Curcuma amada*. To solve the bioavailability issues of mangiferin, it was encapsulated in β-lactoglobulin (β-LG), by desolvation method and reduced to a nano size. From the Dynamic Light Scattering (DLS) data, average particle size and zeta potential of the nanoparticle was 89 ± 10 nm and −30.0 ± 0.2 mV respectively. Scanning Electron Microscopy (SEM) and Atomic Force Microscopy (AFM) results illustrated the spherical and uniform size (approximately 70 nm) of the nanoparticles. The release kinetics of mangiferin by simulated gastrointestinal (GI) studies demonstrated more resistance of nanoparticles towards pepsin digestion in comparison with pancreatin digestion. Release of mangiferin observed in colon fluid was 80%. *In vitro* release kinetics, by Kopcha model, predicted that the mangiferin release from the nanoparticles follows a non-Fickian process. The Baker–Lonsdale model further predicted the spherical shape of the nanoparticles. The nanoparticles can be stored for 30 days at 4 °C retaining its activity. DPPH assay proved that nanoencapsulation of mangiferin retained the antioxidant property. Nanoparticles demonstrated anti-microbial activity against *Staphylococcus aureus* and *Escherichia coli.* No toxicity was observed towards the useful probiotic strain of gastrointestinal tract. The study could establish that the mangiferin/β-lactoglobulin nanoparticles might be a promising candidate for oral delivery.

1. Introduction

The plant based bioactive compounds are used in several nutraceutical and pharmaceutical industries owing to its health applications. Mangiferin, a xanthone in nature extracted from various sources like *Mangifera indica*, leaves of *Arrabidaea patellifera*, *Bombax malabaricum*, *Bombax ceiba*, *Swertia, Mangifera zeylanica*, *Cyclopia genisloides*, root-bark of *Hiptage madablota Gaertn* have found to possess biological activities including anti-cancer, antioxidant, cardiovascular protection, neuroprotection and hepatoprotection (Karim and Azlan, 2012).

In this study, mangiferin is extracted from *Curcuma amada* (mango ginger), a plant belonging to ginger family *Zingiberaceae*, with a spate of purported beneficial health benefits. The genus *Curcuma*, a rhizomatous flowering plant, is extensively used in Ayurveda, Siddha, and Unani medicine systems. *Curcuma amada* is used as a therapy for diseases like sprains, bronchitis, asthma, skin diseases and various skin inflammations. Reported benefits of mangiferin range from anti-oxidant, anti-infectious, anti-diabetic, anti-atherosclerotic, and cardiovascular effects to enhanced cognitive brain function (Chandra, 2017).

Bioactive compounds when passed through gastro intestinal tract are exposed to various adverse conditions like drastic change in pH, which would change the physical state and chemistry of nutraceuticals. To recuperate the efficacy of these bioactive compounds in humans, oral bioavailability of bioactive compounds can be increased by nanoencapsulation (Larsson et al., 2012; Luo et al., 2011). Nanotechnology has crucial importance in the production of novel materials and structures for the applications in food, nutraceutical and pharmaceutical industries (Jahanshahi and Babaei, 2008; Malsuno and Adachi, 1993). These nano-scaled systems have immense benefits, which include enhanced water solubility, increased resistance against chemical degradation, improved absorption in the human body, prolonged circulation, controlled release, elevated cellular uptake and target-specific delivery (Gonza, 2007; Zuidam and Shimoni, 2010). For the purpose of retaining the activity of bioactive compounds like mangiferin, several nanoparticles have been developed. Encapsulation of nutraceuticals in nano polymer assures the protection as well as improves their effectiveness and thereby can be used in site directed targeting. Hence, it is worthwhile to investigate the ability of mangiferin to act as a nutraceutical given a proper delivery vehicle.

For the oral delivery of nutraceuticals, biocompatible polymers used are polysaccharides, lipids, proteins and surfactants (Jones et al., 2011; Luo, Teng, & Wang, 2012). The bioavailability of poorly absorbed drugs can be significantly upgraded by the approach of nanoencapsulation. (Chen et al., 2006; Teng et al., 2016). A polymer or multiple layers of

* Corresponding author.
E-mail addresses: rohinisamadarsh@gmail.com (R. Samadarsi), debjani.dutta@bt.nitdgp.ac.in (D. Dutta).

https://doi.org/10.1016/j.jfoodeng.2018.11.020
Received 28 August 2018; Received in revised form 15 October 2018; Accepted 26 November 2018
Available online 28 November 2018

polymers in the presence of certain stimuli (e.g., pH, organic solvent, temperature, electrolytes) evidently possess the ability to assemble spontaneously into nano-scale matrices. The nano-encapsulation techniques primarily focus on taking advantage of this particular ability of polymers. The nutraceuticals being encapsulated are either insoluble or unstable in the free standing from. Through any of these natural molecular and sub-molecular interactions, such as electrostatic attraction, hydrophobic interaction, hydrogen bonding, and van der Waals force, the bioactive compounds associate with the polymeric matrix and try to attain stability. The range of food and pharmaceutical compounds, which are encapsulated into polymeric nanoparticles, is infact wide spread and diverse as it varies from natural colorant to anti-cancer drugs, from vitamins to antimicrobial agents. By establishing methods for a precise selection of the matrix composition and adequate-tuning of the environmental parameters, the preparation of bioactive compound-loaded particles can be efficiently carried out with an average size of 50–500 nm, together with narrow size distribution and desirable dispersion stability. These nano-scaled systems positively alter the compounds with numerous benefits, which include enhanced water solubility, increased resistance against chemical degradation, improved absorption in human body, prolonged circulation, controlled release, elevated cellular uptake and target-specific delivery (Gibbs et al., 1999; Gonza, 2007; Zuidam and Shimoni, 2010).

β-Lactoglobulin (β-LG) is one of the most abundant whey proteins present in milk of mammalian species. Being a lipocalin protein, β-LG can bind to many hydrophobic molecules and hence plays a vital role in their transport. Bovine β-LG is a small protein of size 3.6 nm and molecular weight of 18.4 kDa with 162 amino acid residues (Sakurai and Oobatake, 2001). The native structure of β-LG protein in solution can be destabilised by various conditions like temperature, pH or ionic strength. Proteins undergo aggregation triggering the formation of transparent `fine-stranded' gels. The protein molecules assemble to form long stiff fibres under prolonged heating at low pH and low ionic strength (Haug et al., 2009). These unique properties make β-LG a natural carrier for oral delivery of mangiferin. In addition, β-LG also exhibits a significant resistance to digestion by pepsin in stomach owing to its rigid β-sheet structures and globular conformation. But, it is digested by trypsin in small intestine (Saadati and Razzaghi, 2012). These unique characteristics of β-LG make it a very efficient oral-based delivery system for the controlled release of mangiferin. Though works have been carried out on encapsulation of bioactive compounds like curcumin (Sari et al., 2015; Teng et al., 2016), and EGCG (Liang et al., 2017) on β-LG protein, encapsulation of mangiferin in β-LG protein by desolvation method is reported for the first time in this study.

Hence this study is focused on the encapsulation of mangiferin in β-LG protein and then reducing its size. Stability of nanoparticles at three different pH levels (3, 4.5 and 7) and two different temperatures (63 °C and 95 °C) were studied. Morphological examinations were carried out using both Scanning Electron Microscopy (SEM) and Atomic Force Microscopy (AFM). SEM was used to determine the final shape of the nanoparticles and AFM was used to reveal the structural properties of the final shape of the nanoparticles. The characterization of the nanoparticles was also conducted by FTIR analysis. The *in-vitro* release mechanism of mangiferin from the nanoparticle under simulated gastro intestinal tract was also studied both by kinetic and thermodynamic methods at 37 °C. Finally the antibacterial activity as well as the microbial toxicity analysis of the nanoparticles was also carried out. This study focuses on improving bioavailability of mangiferin through nanoencapsulation technology for its use as a nutraceutical.

2. Materials and methods

2.1. Materials

Mango ginger (*C. amada*) was purchased from Durgapur, India. The rhizomes were washed, sliced and dried in a hot air oven (OVFU, India) at 60 °C for 72 h and powdered in a grinder. Mangiferin standard was obtained from Sigma Aldrich, USA. The mangiferin extraction was carried out described by Kullu et al. (2014) method with major modifications. Ultrasound-assisted extraction (UAE) (Labsonic P sonifier from Sartorius (Germany)) with acetone as a solvent was used to extract mangiferin from *C. amada.* Extractions were carried out with 75% acetone concentration, solvent-to-solid ratio of 10:1, 80% amplitude, 0.9 W/s duty cycle and 6 min extraction time. The clear solution of *C. amada* extract obtained after UAE was evaporated in a Rotary Vacuum Evaporator (Yamato, Japan), filtered and separated to remove other inactive molecules using chloroform and butanol. The final purified extract was evaporated and dissolved in DMSO and analysed with a UV–vis spectrophotometer (UV-2310, Techcomp), at a wavelength of 410 nm. Mangiferin was estimated by a method followed by Joubert (2012). All of the extractions were carried out in triplicate. Purity of the sample was determined using LCMS analysis (310-MS LC/MS, Triple quadrupole Mass Spectrometer, Agilent Technologies).

2.2. Preparation of β-LG/mangiferin nanoparticles

β-LG nanoparticles with GA and TPP as the cross linkers were prepared by desolvation technique by the method described by Ko and Gunasekaran (2006) with slight modification. Mangiferin at different concentration was added to the 1 mg/ml of β-LG solution. Prepared nanoparticles were stored at 4 °C in acetone for further analysis.

2.3. Determination of encapsulation efficiency

Nanoparticles were centrifuged at 4 °C for 1 h at 8000 rpm. To evaluate the encapsulation efficiency, the supernatant was collected and measured for its total mangiferin content. Total mangiferin content of nanoparticles and permeate was assayed by aluminium Chloride method (Joubert, 2012). Encapsulation efficiency [EE] % was determined by the following equation (Eq. (1)).

$$EE\,(\%) = \frac{\text{Initial amount of mangiferin taken} - \text{Amount of mangiferin in the supernatant}}{\text{Initial amount of mangiferin taken for loading studies}} \times 100 \quad (1)$$

2.4. Nanoparticle characterization

2.4.1. Determination of particle size (PS) and polydispersity index (PDI)

Dynamic light scattering (DLS) spectroscopy (Zetasizer Nano ZS, Malvern Instruments, U.K) was used at 25 °C, and a scattering angle of 90° to measure PS and PDI after dilution of samples with Milli-Q water. Experiment was done in triplicate.

2.4.2. Scanning Electron Microscopy (SEM) analysis

SEM (Carl Zeiss AG - SUPRA 55VP) was used for morphological examination of nanoparticles. The nanoparticles suspension was placed on an aluminum stub and dried under a vacuum for 3 h. Samples were analysed at 20 kV acceleration voltages, after the gold sputtering under an argon atmosphere.

2.4.3. Atomic force microscopy (AFM) analysis

AFM is used to analyse the size and morphology of β-LG nanoparticles. AFM scans topological shape of a specimen without any artefact. An AFM (AIST-NT Smart SPM 1000) system was used under tapping mode to measure size and topological shape of β-LG/mangiferin nanoparticles. The β-LG nanoparticles prepared were spread onto a mica surface and dried in air.

2.4.4. Fourier transform infrared spectroscopy (FTIR)

The composition of the mangiferin and nanoparticles was analysed

by FTIR- 8300 spectrophotometer (Shimadzu, Japan) at a resolution of 4 cm^{-1} in KBr pellets, in the range 400–4000 cm^{-1}.

2.5. Determination of stability of nanoparticle under different processing conditions

The effect of heating (63 °C for 30 min and 95 °C for 10 min) and pH (3, 4.5 and 7) on nanoparticles was studied. The particle size distribution and zeta potential were determined after each treatment by using DLS spectroscopy (Zetasizer Nano ZS, Malvern Instruments, U.K) at 25 °C and scattering angle of 90°(Sari et al., 2015; Teng et al., 2016).

2.6. Determination of storage stability of nanoparticle

Mangiferin nanoparticles were stored at different temperatures (4 °C, 25 °C and 40 °C) for 30 days. Size of the nanoparticles was determined by DLS spectroscopy (Zetasizer Nano ZS, Malvern Instruments, U.K) at 25 °C and scattering angle of 90° at 10 days interval. Amount of mangiferin degraded from the nanoparticles was determined by the method of Joubert (2012).

2.7. In-vitro release study of mangiferin nanoparticles

The mangiferin release from the nanoparticles using dialysis bag was performed by the protocol of Souder and Ellenbogen scheme (Souza, 2014) and was in accordance with the reports of Hurkat et al. (2012); Mcconnell et al. (2008). *In vitro* release of β-LG/mangiferin nanoparticles in the filter unit were collected and used for the determination of the *in vitro* release profile. The samples were dispersed in simulated gastric fluid (SGF) or the simulated duodenum fluid (SDF) or the simulated terminal ileum fluid (STIF) or the simulated colon fluid (SCF), which was immediately placed in the dialysis bags (MWCO 3.5 kDa). The mass ratio between β-LG and pepsin was 20: 1 (w/w) in the simulated duodenum fluid (SDF), the simulated terminal ileum fluid (STIF) and the simulated colon fluid (SCF). SIF is mainly composed of 50 mM PB (pH 6.5) with 0.2% pancreatin and 0.25% bile salts. For gastric digestion, the dialysis bags containing SGF were put in acid release medium I (0.1 M HCl, pH 1.2). pH 4.5 was chosen to simulate the duodenum fluid after emptying substances from the stomach to the small intestine; this pH level also represents the gastric fluid mixed with the upper small intestine fluid. For intestinal stage, the dialysis bags containing STIF were put in release medium II (50 mM PB, pH 7.5). pH 7.0 was selected to simulate the colon fluid (Ghalandari et al., 2014). The dissolution mediums of SGF were simulated for 1 h, SDF for 2–3 h, STIF for 4–5 h and SCF 6–8 h respectively. Aliquots of dissolution medium (0.5 ml) were withdrawn at each time interval, and the obtained released results were analysed for mangiferin release at 410 nm (Eppendorf-3100) using Joubert (2012) estimation method.

2.8. Antioxidant activity of mangiferin nanoparticles

The antioxidant activities of standard mangiferin, unencapsulated β-LG nanoparticles and β-LG/mangiferin nanoparticles were determined by a method proposed by Li et al. (2012) with slight modifications. Briefly, a stock solution of DPPH (0.1 mM) was prepared in absolute ethanol and 0.1 ml of sample solution was added in 2.9 ml of DPPH stock solution. The reaction mixture was incubated in dark at room temperature for 30 min, and the absorbance was measured at 517 nm. The control solution contained the same amount of buffer and DPPH radical. The scavenging activity (SA) % was calculated using equation (Eq (2)).

$$SA\ (\%) = 100(1 - Asample/Acontrol)) \quad (2)$$

Where, $A_{sample,}$ and $A_{control}$ represent the absorbance of the sample reaction and the absorbance of control reaction at 517 nm respectively.

2.9. Antimicrobial activity and microbial toxicity assessment of β-LG/mangiferin nanoparticles

Microorganisms were procured from IMTECH, Chandigarh, India. Antimicrobial activity of β-LG/mangiferin nanoparticles was evaluated against the following microorganisms like *E. coli (Escherichia coli)* (MTCC-739), *Bacillus subtilis* (MTCC-441), and *Staphylococcus aureus* (MTCC-96). Microbial toxicity of nanoparticles was studied on probiotic strains of intestinal flora like *Lactobacillus acidophilus* (MTCC-5401), *Bacillus subtilis (MTCC-441), Lactobacillus rhamnosus* (MTCC-5897) and *Escherichia coli* (JM105 K-12) strains by agar disc diffusion method. (M02-A12: Performance Standards for Antimicrobial Disk Susceptibility Tests; Approved Standard—Twelfth Edition, 2015). The β-LG/mangiferin nanoparticle solution was prepared at a concentration of 400 μg/disc. The nanoparticle was infused into the paper discs and placed onto the agar media inoculated with the test bacteria and incubated at 37 °C for 24 h. Mangiferin (400 μg/disc) and unencapsulated β-LG nanoparticle were used as controls. After incubation, zone of inhibition formed around the disc was examined and assessing the antimicrobial activity on the basis of measurement of diameter of the inhibited zone formed around the disc (Krishnan et al., 2015).

2.10. Preparation of inoculum

Stock plates were maintained at 4 °C on slopes of nutrient agar, MRS agar and Luria Bertani agar. Active cultures for experiments were prepared by transferring a loopful of cells from the stock cultures to test tubes of nutrient broth for *Staphylococcus aureus,* MRS broth for *Lactobacillus acidophilus and* Luria Bertani (LB) broth for *Bacillus subtilis and Escherichia coli* were incubated without agitation for 24 h at 37 °C respectively. To 50 ml of nutrient broth and LB broth 5.0 ml of culture was inoculated and incubated till it reached the turbidity equal to that of the standard 0.5 McFarland solution at 600 nm which is equivalent to 10^6–10^8 CFU/ml (Balouiri et al., 2016; Nijs et al., 2003).

The antimicrobial efficacy of β-LG/mangiferin nanoparticles was examined using the standard broth dilution method (CLSI M07-A8). The MIC was determined in broth using serial two-fold dilutions of β-LG/mangiferin in concentrations ranging from 0.132 mg/ml to 10 mg/ml with adjusted bacterial concentration (0.10 at 625 nm (1.108 CFU/ml, 0.5 McFarland's standard) (Krishnan et al., 2015). The positive control used in this study contained broth medium with tested bacterial concentrations and negative controls were mangiferin inoculated broth and β-LG inoculated broth respectively. The cultures are incubated for 24 h at 37 °C. The MIC was observed by the visual turbidity of the tubes both before and after incubation and it was done in six sets to confirm its value for the tested bacteria. After the MIC determination of the β-LG/mangiferin nanoparticles, aliquots of 50 μl from all tubes which showed no visible bacterial growth were seeded in agar plates, which were not supplemented with nanoparticles, were incubated for 24 h at 37.C. The MBC was observed for presence or absence of bacterial growth in agar plates both before and after incubation.

2.11. Statistical analysis

In this study all samples were prepared and analysed in triplicate. The data was presented as means ± standard deviations of three determinations. Statistical differences between two groups were evaluated using the Student's *t*-test. Multiple comparisons of means were done by LSD (least significant difference) test. A probability value of < 0.05 was considered significant. All statistical analysis was done using windows V8.

3. Results and discussion

3.1. Mangiferin extraction from curcuma amada

Chromatographic profile of the mangiferin extracted from *Curcuma amada* by UAE treatment and standard mangiferin is given in Fig. 1. The retention time, 1.75 min of the extract was well in accordance with the standard which confirms the presence of mangiferin in *Curcuma amada* extract. The purity of obtained extract was 99.99%

3.2. Optimization and characterization of mangiferin nano particles

3.2.1. The size and zeta-potential of prepared nanoparticle

In the present study, preparation of nanoparticles was achieved by both β-LG and denatured β-LG, to obtain a stable formulation, by de- or anti-solvation (Teng et al., 2015). In water, the β-LG molecules exist as folded globular forms with exposed negatively charged groups to the solvent. The addition of an antisolvent like acetone enhances the partial protein unfolding, which exposes its hydrophobic sites that are previously buried in the region. The surface charge of the protein is reduced by the antisolvent, which competes for water molecules with β-LG leading to the increase in hydrophobic association and reduction in electrostatic repulsion, both of which facilitate protein aggregation. Nutraceuticals like mangiferin can be encapsulated into the protein dispersion by dissolving the compound into the antisolvent. The desolvation process can be reversed by adding sufficient water, which leads to the dissociation formed particles into individual molecules as the solvent polarity increases. Two types of crosslinkers were used for the preparation of nanoparticles, glutaraldehyde (GA) and tripolyphosphate (TPP) (Table 1). Crosslinking was achieved by both ionic crosslinking (physical crosslinking) using TPP and covalent crosslinking (chemical crosslinking) using GA, in which particle integrity can be retained.

The two aldehyde groups on GA react with two primary amine groups on adjacent lysine residues of the protein, creating a covalent bond that maintains the particle structure. As the antisolvent, is removed the morphology of the nanoparticles is retained and they do not dissociate into individual molecules. GA is widely used for crosslinking and stabilization of protein derived nanoparticles due to its low cost production, great fixation and for the controlled drug release rate (Andriani and Grastianto, 2015). Initially the nanoparticles were prepared with GA as a crosslinker to determine the encapsulation efficiency of β-LG/mangiferin nanoparticles. The concentration of GA used was insignificant (0.016 mg/ml) to cause toxicity. The size of β-LG/mangiferin nanoparticle with GA as the cross linker, was observed to be 308 ± 10 nm ($P < 0.05$) and −30.0 ± 0.2 mV ($P < 0.05$) respectively (Table 1). To attain reduction in particle size, native β-LG protein was heat denatured and the nanoparticles were prepared again with GA as the crosslinker. From the present study it was observed that the size of the nanoparticle increased at high temperature which might be caused by the denaturation of β-LG which leads to aggregation (Table 1). On temperature treatments above 70 °C, the dimmers of β-LG, dissociate into monomers (Teng et al., 2015) followed by some crucial change in the conformation of the β-LG monomer. These changes lead to the exposure of hydrophobic groups and the free sulphydryl group (Cys121) (Relkin, 1998), resulting in a reactive monomer which can propagate an aggregation reaction leading to the formation of non-native dimers, trimmers, tetramers and larger aggregates by polymerization. It was observed that denatured β-LG did not show a positive result with respect to their size as the size increased from 308 nm to 890 nm ($P > 0.05$) due to aggregation and zeta potential reduced to −19.0 ± 0.2 mV ($P > 0.05$) (Table 1). Encapsulation efficiency of denatured β-LG nanoparticles was 65% which was less in comparison with non-denatured β-LG nanoparticles (Table 1).

A desirable size was not achieved by using GA, as it formed covalent bonds with β-LG possibly causing a structural change in β-LG. Hence an alternative method of crosslinking using tripolyphosphate was adapted. Physical crosslinking of TPP with β-LG was based on the interactions (ionic) between charged β-LG and TPP (Stoica and Ion, 2013). Reversibility was achieved by using TPP and is considered to be good in biocompatibility due to the deficient usage of harsh preparation condition.

β-LG/mangiferin nanoparticle with TPP as the cross linker had a particle size of 89 ± 10 nm ($P < 0.02$), zeta potential of −30.0 ± 0.2 mV ($P < 0.03$) and poly dispersity index (PDI) of 0.203 (Table 1). The surface of β-LG was found to have positive and negative charges. Therefore, the electrostatic interactions between the positively charged group of β-LG and negatively charged groups of

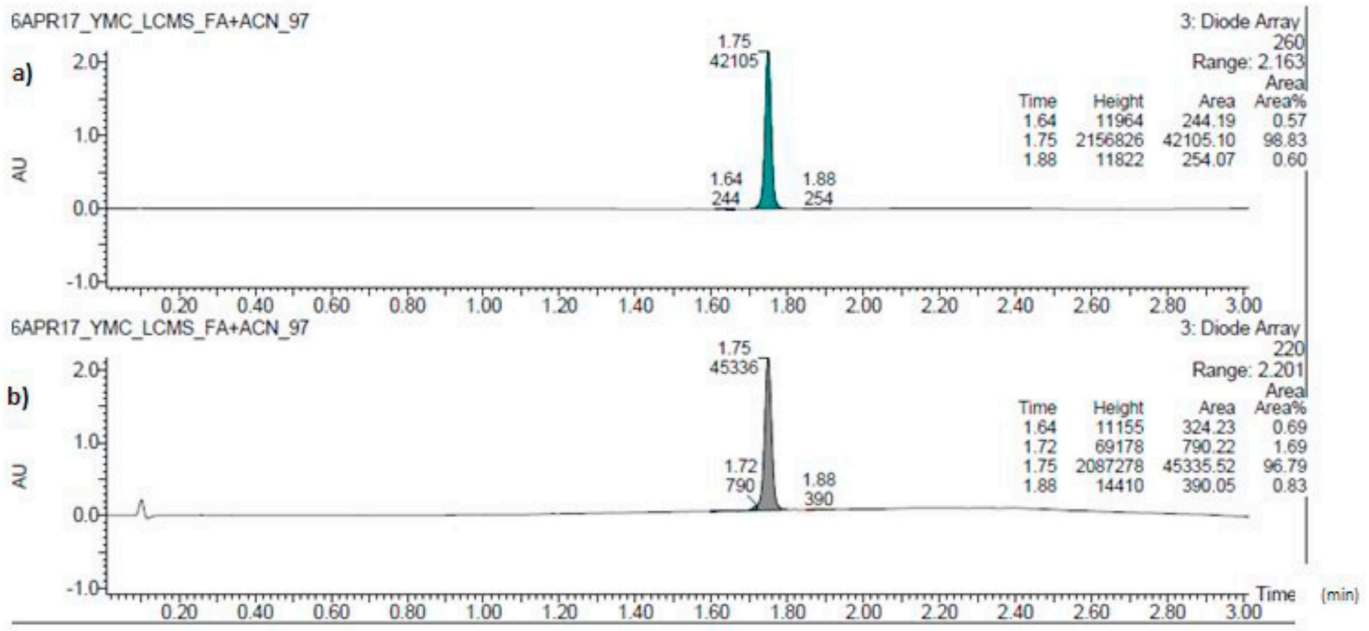

Fig. 1. Chromatographic profile (UPLC/MS) (a) mangiferin extracted from *Curcuma amada* by UAE treatment and (b) standard mangiferin.

Table 1
Physico-chemical characteristics of mangiferin nanoparticles.

Nanoparticle Composition	Concentration of mangiferin (μg/ml)	Size (nm)	Zeta Potential (mV)	PDI	Maximun EE (%)
β-LG (2 mg/ml)/Mangiferin Nanoparticle with Gluteraldehyde (0.032 mg/ml) as cross-linker	450	308 ± 10	−33.0 ± 0.2	0.27	88
Denatured β-LG (1 mg/ml)/Mangiferin nanoparticle with GA (0.016 mg/ml) as the cross linker	400	890 ± 10	−19.0 ± 0.2	0.3	65
β-LG (1 mg/ml)/Mangiferin nanoparticle with TPP (0.12 mg/ml) as cross-linker	**400**	**89 ± 10**	**−30.0 ± 0.2**	**0.2**	**85**

Table 2
Effect of heating on particle size and zeta potential in β-LG/mangiferin(400 μg/ml) nanoparticle with TPP(0.12 mg/ml) as the cross linker.

Temperature	Average Particle Size (nm)	Zeta Potential (mV)
Room temperature	89 ± 10 nm	−30.0 ± 0.2
Pasteurization	95 ± 8 nm	−21.0 ± 0.6
Boiling	304 ± 9 nm	−20.0 ± 0.6

tripolyphosphate played a crucial role in encapsulating mangiferin as well as the particle size reduction of the nanoparticle. Zi Teng et al., 2015 has reported that nanoparticles with zeta potentials either above +30 mV or below −30 mV are found to possess good stability in dispersions, due to the significant electrostatic repulsion between them. Luo et al., 2012 and Luo et al. (2011) in their study have observed that the soya protein nanoparticles with high zeta potential are utilised as a second coating layer that improves the dispersion stability when poorly charged materials like zein are used for encapsulation. In the present study when β-LG/mangiferin nanoparticles with TPP as the cross linker has a high zetapotential value of −30.0 ± 0.2 mV (Table 2) which could also indicate their stability in dispersions.

In β-LG/mangiferin nanoparticles, the net negative zeta potential might be due to the existence of TPP used in formulations, hence the surface charge is contributed not only by β-LG but also by TPP. The repulsive forces among the nanoparticles resulted in the stability of nanoparticles. Since stability and desired particle size was obtained with 400 μg/ml of mangiferin, 1 mg/ml β-LG and 0.12 mg/ml TPP (Table 1), further work was carried out at this concentration.

3.2.2. Morphology analysis of mangiferin encapsulated nanoparticles by SEM and AFM

The SEM results demonstrated that the nanoparticles were spherical, homogeneous, and uniform in size (Fig. 2). The particle sizes were found to be approximately 70 nm, which was less when in comparison with DLS data (Table 1), this might be due the fact that measurement was taken in the dry state in the case of SEM, which caused the nanoparticles to shrink. The results were further confirmed by the AFM results (supplementary data) which implied that the nanoparticle was spherical and uniform in size and shape as well. The size of nanoparticles was approximately 100 nm, which allows better absorption and release by providing high diffusion conditions. In the present study, results were in accordance with the reports of Ghalandari et al. (2014); Ko and Gunasekaran (2006); Luo et al. (2011).

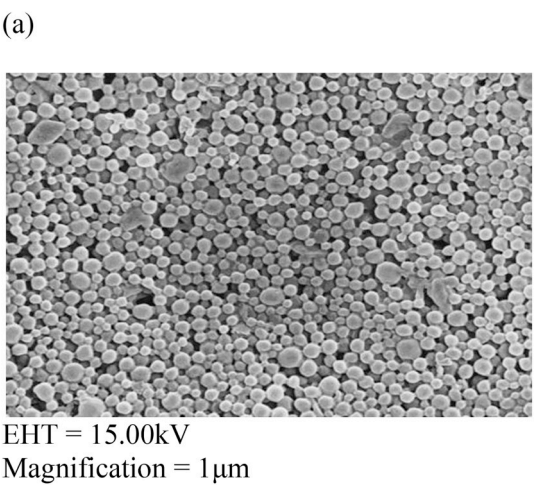

Fig. 2. SEM image of β-LG/mangiferin nanoparticles with TPP as the cross linker.

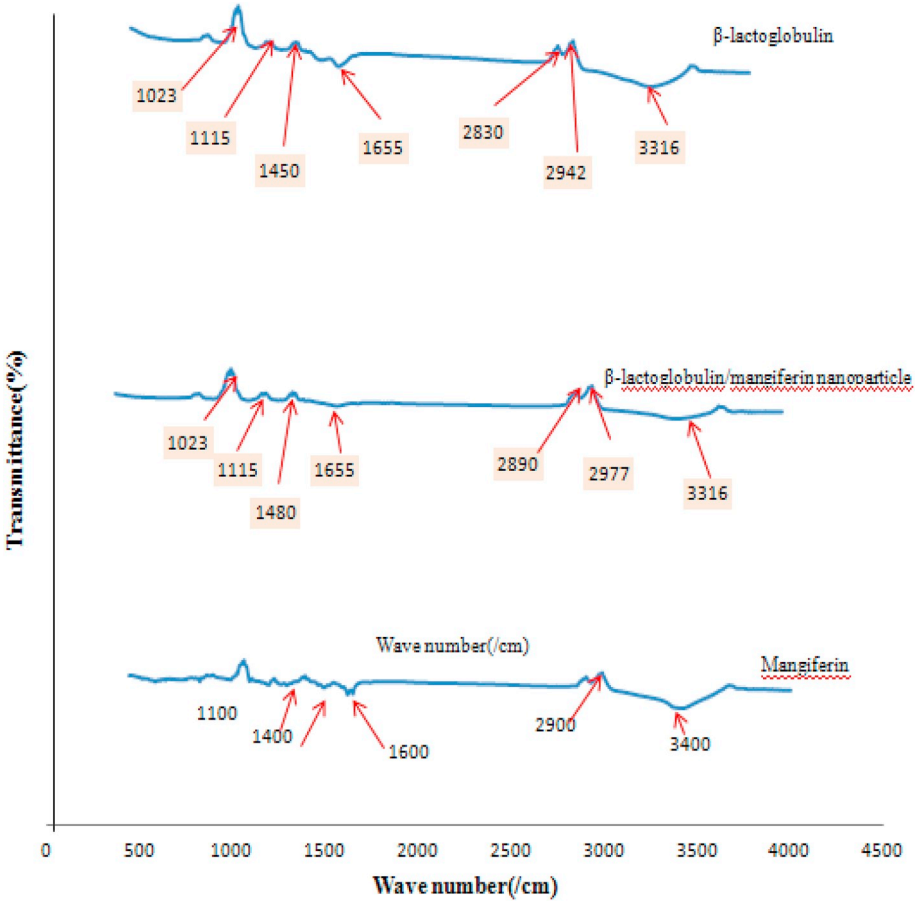

Fig. 3. Fourier-transform infrared spectroscopy analysis of mangiferin, β-LG/mangiferin nanoparticle and unencapsulated β-LG nanoparticles.

3.2.3. Fourier-transform infrared spectroscopy

FTIR analysis is an analysis technique for the characterization and identification of compounds or functional groups (chemical bonds). Identification and estimation of secondary structures of the native protein and subsequent change in both secondary and tertiary structures was studied. These changes were due to interactions with other molecules like mangiferin and TPP (Fig. 3.).

To study the encapsulation mechanism of mangiferin in β-LG nanoparticle investigation was done using FTIR technique. Each functional group absorb unique energy and produce distinct characteristic peak at FTIR spectrum (Saha et al., 2016). These peaks can be studied to identify the functional groups present on the nanoparticle surface and to predict the mechanism of mangiferin encapsulation (Fig. 3).

FTIR spectrum of β-LG (Fig. 3) revels the existence of carbon-carbon (C-C), carbonyl(C = O), carbon-carbon (CH-CH), carbon-oxygen (C-O), carbon-hydrogen(C-H) and hydroxide (O-H) groups on the surface. The broad spectrum at 1023 cm^{-1} and sharp peak at 3316 cm^{-1} can be attributed due to C-C stretching and O-H secondary structure respectively. Peak at 1115 cm^{-1} is due to C = Oat 1450 cm^{-1} due to CH-CH, broad peak at 1655 due to C-O stretching, medium peak at 2830 cm^{-1} due C-H (symmetric) and at 2942 cm^{-1} due to C-H(asymmetric) (Li et al., 2012).

FTIR spectrum of β-LG/mangiferin nanoparticle reveals the habitation of carbon-carbon (C-C), carbonyl (C = O), carbon-carbon (CH-CH), carbon-oxygen (C-O), carbon-hydrogen (C-H) and hydroxide (O-H) groups on the surface. On comparing with unencapsulated β-LG and β-LG/mangiferin nanoparticles it was observed that at 1480 cm^{-1} (CH-CH),2890 $cm^{-1,}$ (C-H (symmetric)), and 2977 cm^{-1} (C-H (asymmetric)) peaks showed variation which might be responsible for the encapsulation of mangiferin inside the nanoparticles (Fig. 3). Significant shifting in the distinctive peaks of the OH group or amide group (Fig. 3) was not observed, hence it could be concluded from the FTIR study that β-LG was not conjugated to mangiferin nanoparticles through covalent bonding. The FTIR spectra of mangiferin-β-LG nanoparticles presented characteristic peaks at 1023, 1115, and 3316 cm^{-1},which is hard to be assigned to any mangiferin related stretching vibration (Teng et al., 2016). From the FTIR results (Fig. 3.), it is proposed that the interactions of mangiferin nanoparticles with β-LG protein is not a covalent interaction but based on physical adsorption. In a study by B. Li, Du, Jin and Du (2012) on Epigallocatechin-3-gallate encapsulated β-LG nanoparticles results observed were similar.

3.3. Stability test of nanoparticles

The difference in particle size and zeta potential of nanoparticles under different processing conditions were studied.

3.3.1. Effect of heating

The effect of heat on the average particle size and zeta potential of β-LG/mangiferin nanoparticle was studied at 63 °C for 30 min (pasteurization) and 95 °C for 10 min (boiling). From Table 2, it was noticed that the nanoparticle size increases from 89 ± 10 nm (control) to 95 ± 8 nm ($P < 0.05$) during pasteurization conditions and 304 ± 9 nm ($P > 0.05$) during boiling. The zeta potential changed from −30.0 ± 0.2 (control) to −21.0 ± 0.6 mV during pasteurization ($P \leq 0.05$) and −20.0 ± 0.6 mV ($P = 0.05$) during boiling respectively. A significant change in the average particle size and zeta potential of the nanoparticles under processing conditions was observed. This was due to the change in the surface charge of the nanoparticles at higher temperature due to the denaturation of β-LG causing

Table 3
Effect of pH on particle size and zeta potential of β-LG/mangiferin(400 μg/ml) nanoparticle with TPP(0.12 mg/ml) as the cross linker.

pH	Particle Size (nm)	Zeta Potential (mV)
3	1012 ± 12 nm	−09.0 ± 0.24
4.5	337 ± 12 nm	−10.0 ± 0.10
9	89 ± 10 nm	−30.0 ± 0.2

the monomer formation and the increase in nanoparticle size (Teng et al., 2016). Sari et al. (2015) studied the influence of temperature on the stability of curcumin encapsulated whey protein nanoemulsions and concluded that the nanoemulsions were prone to aggregation at elevated temperatures.

3.3.2. Effect of pH

The particle size and zeta potential of the nanoparticles was determined at pH 3.0, pH 4.5 and pH 9 and is given in Table 3.

There was a significant difference in the zeta potential of the nanoparticles with change in pH from 3.0 to 9.0. ($P > .0.05$). The isoelectric point of β-LG is 5 (Teng et al., 2016). The particles at pH 4.5 had a surface charge −10.0 ± 0.10 mV in comparison with the particles at pH 9.0 (−30.0 ± 0.17 mV) ($P > 0.05$) (Table 3). This is might be due to the reason that the surface charge of the β- LG protein shifts to positive at pH below its isoelectric point. This shift in the zeta potential indicates that the surface charge of the prepared nanoparticles is contributed mainly by β- LG proteins. Rao and Mcclements (2011) studied the impact of nano/microemulsions on various environmental stress and found that relatively stable nanoemulsions were formed at pH 6.0 and 7.0, but extensive particle growth/aggregation occurred at lower and higher pH values, which was attributed to either chemical (hydrolysis) or physical (electrical charge) effects. The reduction in the electrical charge on the particles at lower pH value would reduce the electrostatic repulsion between them, thereby leading to aggregation (Rao and Mcclements, 2011). However in the prepared nanoparticle using β-LG and mangiferin, a stable nanoparticle was formed at pH 9, which was a deviation from the studies of Rao and Mcclements (2011).

3.4. Storage stability studies

Temperature is a crucial parameter for the nanoparticle stability during storage. High temperature leads to the increase in particle collision frequency, promoting aggregation under certain conditions (Zhao et al., 2018). The stabiliyof β-LG/mangiferin nanoparticles were studied for a period of 30 days at storage conditions 4Ί C, 25Ί C and 40Ί C at 10 days interval, with respect to mangiferin degradation (Fig. 5.) The change in the size and zeta potential of the nanoparticles was also studied with respect to DLS data (Table 4 and Fig. 4.). The nanoparticle was stable for 30 days at 4 °C, but showed a slight increase in particle size at 25 °C and 40 °C. The average particle size at 4 °C increased slightly from 89 ± 10 nm to 92 ± 10 nm ($P < 0.05$) when kept for storage for 30 days (Table 4 and Fig. 4b). There was very slight decrease in the magnitude of zeta potential ($P < 0.05$) of the nanoparticles (Table 4). For the nanoparticles kept at room temperature, average particle size increased from 89 ± 10 nm (Fig 4a) to 94 ± 10 nm ($P < 0.05$) (Table 4 and Fig. 4c). Mangnitute of zeta potential decreased from −30.0 ± 0.2 mV to −25.0 ± 0.2 mV ($P < 0.05$) (Table 4). However when the nanoparticles were kept at 40 °C the particle size increased from 89 ± 10 nm (Fig. 4a) to 97 ± 10 nm ($P < 0.05$) (Table 4 and Fig. 4d). Negligable amount of mangiferin was degraded at 4 °C (2.34%) ($P < 0.002$) and 18% ($P < 0.05$) mangiferin degradation was observed at 40 °C (Fig. 5.), which was probably because of the occasional light exposure, a factor that could degrade mangiferin slightly (Kawakami and Gaspar, 2015). The relatively lower value of PDI for nanoparticles kept for storage was probably because of

Table 4
Storage stability studies on β-LG/mangiferin Nanoparticles.

Temperature	Number of days									
	0 day		1 day		10 days		20 days		30 days	
	Particle Size (nm)	Zeta Potential (mV)	Particle Size (nm)	Zeta Potential (mV)	Particle Size (nm)	Zeta Potential (mV)	Particle Size (nm)	Zeta Potential (mV)	Particle Size (nm)	Zeta Potential (mV)
4 °C	89 ± 9 nm	−30.0 ± 0.2 mV	89 ± 9 nm	−30.0 ± 0.2 mV	89 ± 10 nm -	−30.0 ± 0.2 mV	92 ± 10 nm	−29.0 ± 0.2 mV	92 ± 10 nm	−28.0 ± 0.2 mV
25 °C	89 ± 9 nm	−30.0 ± 0.2 mV	92 ± 9 nm	−28.0 ± 0.6 mV	93 ± 9 nm	−28.0 ± 0.6 mV	94 ± 9 nm	−27.0 ± 0.6 mV	94 ± 9 nm	−25.0 ± 0.6 mV
40 °C	89 ± 9 nm	−30.0 ± 0.2 mV	95 ± 9 nm	−24.0 ± 0.6 mV	96 ± 9 nm	−23.0 ± 0.6 mV	97 ± 9 nm	−22.0 ± 0.6 mV	97 ± 9 nm	−22.0 ± 0.6 mV

Experiments were done in triplicates. Data were expressed as Mean ± Standard Deviations (SD).

a)

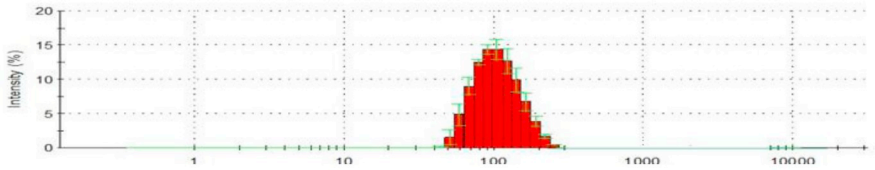

b)

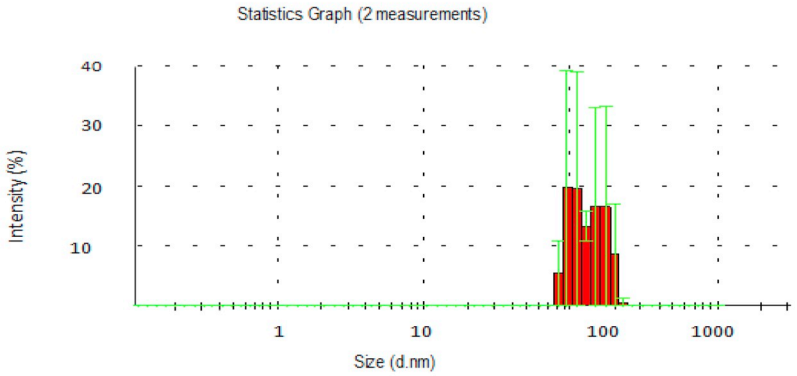

c)

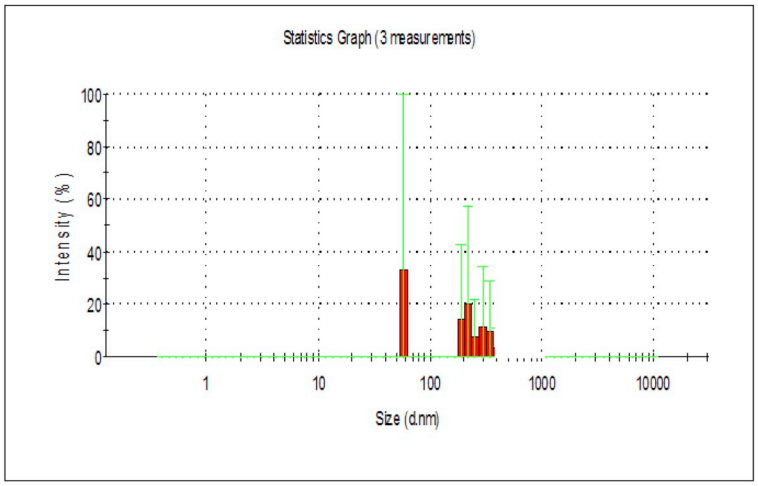

d)

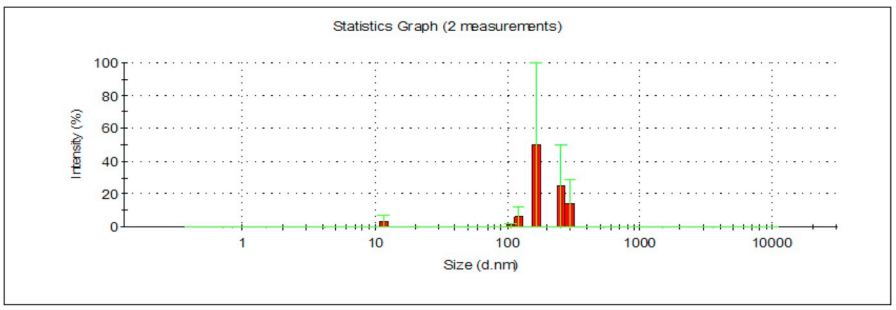

Fig. 4. Storage stability studies of β-LG/mangiferin nanoparticle (a) The average particle size of β-LG/mangiferin initially is 89 ± 10 nm (control), (b) The average particle size of β-LG/mangiferin at 4 °C after 30 days, (c) The average particle size of β-LG/mangiferin at 25 °C after 30 days and (d) The average particle size of β-LG/mangiferin at 40 °C after 30 days.

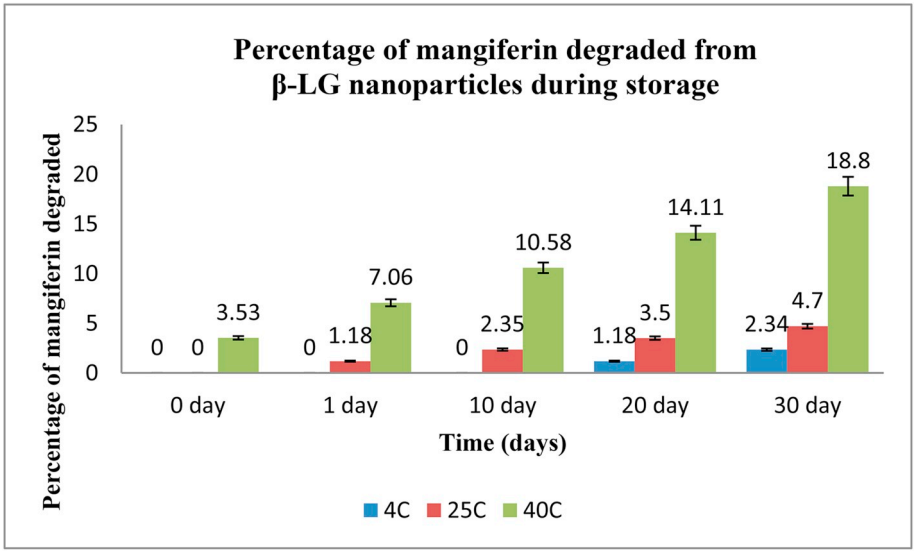

Fig. 5. Percentage of mangiferin degraded from nanoparticles during storage.

the formation of stable nanoparticles. There are no previous reports on mangiferin nanoparticles storage stability studies. The reason for the aggregation of nanoparticles during storage in nanoparticles stabilized by globular proteins is flocculation characterized by the exposure of non-polar groups in the protein, resulting in a change in the surface charge of the protein. (Mcconnell et al., 2008). Partial degradation of β-LG occurring during the storage leads to the exposure of some active sites in the protein, resulting in slight aggregation (Relkin, 1998). From the study, it could be concluded that the mangiferin/β-LG nanoparticles had a good shelf life and 4 °C is the ideal temperature for storage of β-LG/mangiferin nanoparticles.

3.5. In-vitro release study

The release of mangiferin from nanoparticles plays a vital role in the bioavailability. The gastric, intestinal, terminal ileum and colon digest were analysed for release percentage of mangiferin encapsulated nanoparticle.

This study demonstrated that β- LG was resistant towards pepsin digestion. A 9.4% release of mangiferin was observed after gastric fluid (Fig. 6a and b). β- LG is well known for its resistance against pepsin, at pH 1.2. Teng et al. (2015) suggested that complexation with folic acid did not alter the digestion of β- LG in the stomach. This binding is reasonable, since the nutrient binding occurs in the native binding sites of β- LG and does not require a conformational change. Therefore, a controlled release pattern with minimal release in the stomach at pH 1.2 is expected with β- LG/mangiferin nanoparticle. pH 4.5 is near to the iso electric point of β- LG protein. At this pH proteins aggregate further resisting the release of mangiferin. β- LG possesses unique property of resistance against pepsin, the major protease in human's stomach. Factors accounting for such feature are, pepsin cleaves peptide bonds at the hydrophobic patch of protein; however, the peptic digestion of β- LG is limited by its abundance in charged and polar amino acids. In addition, β- LG contains a high content (> 55%) of rigid beta-sheet structure, which reduces its molecular flexibility and prevents pepsin from approaching and associating with the protein. The existence of two disulfide bonds (Cys82–Cys176, and Cys122–Cys135/137 depending on the type of variants) in β- LG further stabilizes the protein structure from dissociation (Teng et al., 2015). Mangiferin is protected by the β-LG nanoparticle at pH 1.2 and pH 4.5, therefore there would be negligible chemical changes occurring with mangiferin. On the other hand, β- LG can be slowly digested by trypsin in the small intestine at pH 7.5. These two digestive properties make β- LG an attractive encapsulant for the controlled release of mangiferin or drugs in the GI tract. Therefore release of mangiferin starts at simulated intestinal fluid (pH 7.5) and continues further at simulated colon fluid (pH 7). Bile salts and the trypsin/chymotrypsin fraction present in pancreatin helped in the breakdown of β-LG and a 75% release of mangiferin (Fig. 6a.) It was observed that in simulated colon fluid, the β-LG/mangiferin nanoparticles were destabilised and approximately 80% of the encapsulated mangiferin was released within 6–8 hrs. The mangiferin release from nanoparticles was high from the terminal ileum fluid and complete digestion occurred in the colon fluid. Thus, the release of mangiferin from β-LG nanoparticles to its target site was pH sensitive.

In the current study, kinetics of the release model explained the release of mangiferin from β-LG nanoparticles and the effective parameters in the release mechanism was determined by thermodynamic studies. In the oral delivery of mangiferin, both approaches are essential. Among thermodynamic parameters that are impressive on mangiferin release process, the Gibbs free energy as describing chemical events has critical role where as the value of it explored the mangiferin transfer from carrier to target place. Hence, Gibbs free energy (ΔG^0_{tr}) values for mangiferin transfer from β-LG nanoparticles were calculated based on Eq. (3) (Ahuja et al., 2007).

$$\Delta G^0_{tr} = -2.303RT\log\left(C_t/C_T\right) \quad (3)$$

Where C_T represents the total concentration of mangiferin and C_t is the concentration of mangiferin in simulated time intervals respectively. R is the gas constant and T is the temperature. The Gibbs free energy of mangiferin release from β-LG nanoparticles was maximum in SCF at pH 7.0 and then in STIF at pH 7.5. Significantly less amount of mangiferin (9.48%) was released from the nanoparticles at pH 1.2 (Fig. 5a). The mangiferin release was higher in SDF when compared to SGF. Nanoparticles were found to resist the mangiferin release in SGF at pH 1.2 and SDF at pH 4.5.

From the time dependency study results (Fig. 6c), the maximum Gibbs free energy of mangiferin release from nanoparticles was observed in SCF during the 8-h interval. Maximum release of mangiferin occurred at 8-h interval in SCF (pH 7) and STIF (pH 7.5) (Fig. 6b). Hence it can be proposed that β-LG nanoparticles containing mangiferin are best suited for colon oral delivery.

The thermodynamics and kinetics aspects of the results have demonstrated that mangiferin release is pH sensitive. The mangiferin release starts in the STIF condition (pH 7.5) and continues in the colon,

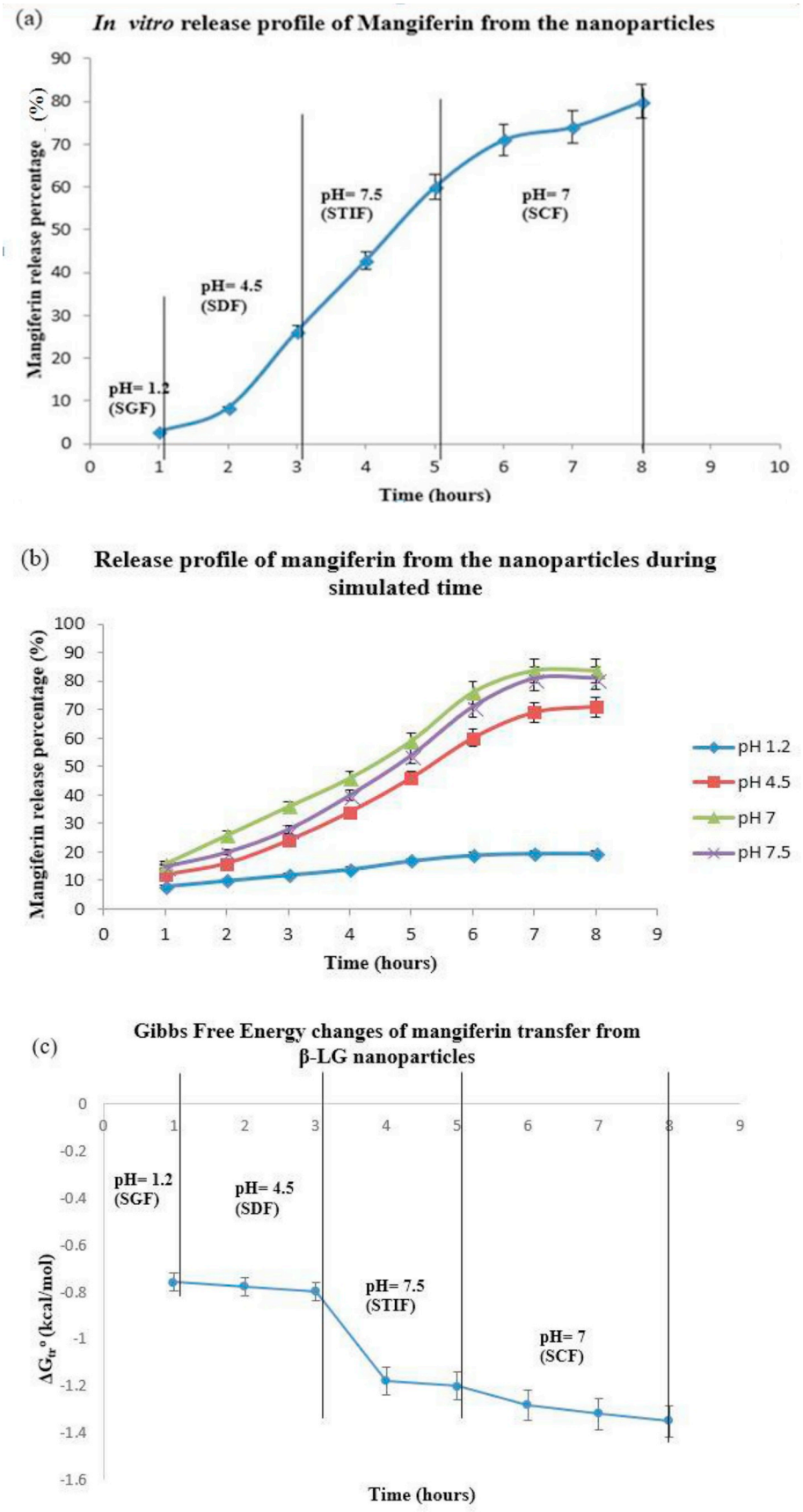

Fig. 6. *In vitro* release of mangiferin from β-lactoglobulin nanoparticles with TPP as the cross linker (a) The release profile of mangiferin from β-LG nanoparticles in simulated gastrointestinal fluid conditions at 37 °C during 8 hrs, (b) Release profile of mangiferin from β-LG nanoparticles in simulated gastrointestinal fluid conditions at 37 °C during simulated time, (c) Plot of Gibbs free energy changes of mangiferin release from β-LG nanoparticles to aqueous solution of simulated gastrointestinal fluid conditions at 37 °C during 8 hrs.

with the highest release taking place in the simulated colon fluid (pH 7.0). The release data was evaluated by fitting a mathematical kinetics model to determine the release kinetics of mangiferin from β-LG nanoparticles. The best model was selected based on the value of the correlation coefficient (R^2) for the fitted results.

Release kinetics were evaluated by the following models of zero-order, first-order (Lobo and Costa, 2001), Weibull (Kosmidis and Argyrakis, 2003), Higuchi (1963), Hixson–Crowell (Hixson and Crowell, 1931) and Korsmeyer–Peppas (Korsmeyer et al., 1983).

Eqs. (4)–(9) were used for the study.

$$\text{Zero} - \text{order model: } M_t = M_0 + k_0 t \tag{4}$$

$$\text{First} - \text{order model: } \log M_t = \log M_0 + \frac{k_1 t}{2.303} \tag{5}$$

$$\text{Weibull model: } \frac{M_t}{M_\infty} = 1 - \exp(-at^b) \tag{6}$$

$$\text{Higuchi model: } M_t = k_H \sqrt{t} \tag{7}$$

$$\text{Hixson} - \text{Crowell model: } \sqrt[3]{w_0} - \sqrt[3]{w_t} = k_{HC} t \tag{8}$$

$$\text{Korsmeyer} - \text{Peppas: } \frac{M_t}{M_\infty} = k_{KP} t^n \tag{9}$$

where t is the release time; M_0 is the amount of mangiferin released at time zero, M_t is the amount of mangiferin released at a time, t, and M_∞ is the amount of mangiferin released at time infinity.

The parameters w_0 is the mangiferin concentration at time zero and w_t is the mangiferin concentration at time t. The parameters k_0, k_1, k_H, k_{HC} and k_{KP} are the release kinetic constants in zero-order, first-order, the Higuchi, Hixson–Crowell and Korsmeyer–Peppas models, respectively. The variables a and b are constants and n represent the release exponent and hence indicates the release mechanism of mangiferin. The correlation coefficient values that were obtained are given in Table 5. In the simulated conditions, the release results are well fitted to the Korsmeyer–Peppas model. In a study by Lobo and Costa (2001) it was observed that Korsmeyer–Peppas model is generally used for drug release from the polymer matrix. Hence, noting the release exponent in Korsmeyer–Peppas model, mangiferin release mechanism from β-LG nanoparticles has a non-Fickian diffusion because the values (Table 6) are between 0.5 and 1 in all of the simulation conditions. Korsmeyer et al., 1983 characterized n value for release mechanisms as $n = 0.5$, $0.5 < n < 1$, $n = 1$ and $n > 1$ representing Fickian diffusion, anomalous (non-Fickian) diffusion (i.e. by both diffusion and erosion, case II transport (zero-order (time-independent) release) and super case II transport, respectively.

In the release of mangiferin from nanoparticles diffusion and erosion processes was found to occur simultaneously. To determine the accurate contribution of diffusion and erosion, the release results were fitted with the Kopcha model (Eq. (10)):

$$Mt = A\sqrt{t} + Bt \tag{10}$$

Where t is the release time, A and B represents the diffusion and the erosion terms, respectively. In the Kopcha model, a large positive number and a large negative number was attained, which suggested an initial burst release and a lag time before releasing from the nanoparticle. Also, A to B ratio (A/B) indicates A and B contribution in release mechanism whereas $A/B = 1$ illustrate that diffusion and erosion are equal, $A/B < 1$ shows that erosion predominates over diffusion, and $A/B > 1$ indicates that diffusion predominates over erosion (Hixson and Crowell, 1931).

Table 5
Comparison between correlation coefficient of release kinetic models.

pH	Zero order R^2	First order R^2	Higuchi R^2	Hixson-Crowell R^2	Weibull R^2	Korsmeyer-Peppas R^2
1.2	0.92	0.64	0.87	0.75	0.8	0.94
4.5	0.90	0.69	0.91	0.76	0.74	0.97
7	0.95	0.8	0.93	0.86	0.69	0.98
7.5	0.74	0.52	0.87	0.59	0.8	0.9

Experiments were done in triplicates. Data were expressed as Mean ± Standard Deviations (SD). Values differ significantly at $P < 0.05$.

Table 6
Release exponent parameter, release mechanism describing parameters and kinetic model for shape characterization of Mangiferin encapsulated β-LG nanoparticles with TPP as the cross linker.

pH	Korsmeyer-Peppas n	Kopcha				Baker-Lonsdale R^2
		R^2	A($\mu g h^{-½}$)	B($\mu g h^{-1}$)	A/B ($h^{1/2}$)	
1.2	0.74	0.98	0.14	3.6	0.033	0.98
4.5	0.65	0.98	0.22	4.9	0.042	0.97
7	0.61	0.98	2.26	14.4	0.152	0.98
7.5	0.74	0.96	2.3	15.2	0.16	0.98

Experiments were done in triplicates. Data were expressed as Mean ± Standard Deviations (SD). Values differ significantly at $P < 0.05$.

The Kopcha model results are given in Table 6. Since the correlation coefficient in Kopcha model was 0.985, it was predicted that the release of mangiferin from the nanoparticles follows the non-Fickian process. This also illustrated that the erosion contribution is maximum for SCF (pH 7.0) and STIF (7.5) when in comparison with SGF (pH 1.2) and SDF (pH 4.5). A/B value is slightly larger at SCF (pH 7) when compared to that at STIF (pH 7.5). At SGF (pH 1.2) and SDF (pH 4.5), mangiferin nanoparticles did not undergo gastric digestion by enzymes, since erosion profile was very low. It could be concluded that the mangiferin encapsulated β-LG nanoparticles with TPP as the crosslinker is ideal for mangiferin to be targeted in the colon fluid from thermodynamic and kinetic studies.

Baker–Lonsdale model was used (Lobo and Costa, 2001) to analyse the shape of nanoparticles in the release using Eq. (11)

$$\frac{3}{2}\left\{1 - \left\{1 - \frac{Mt}{M\infty}\right\}^{2/3}\right\} - \frac{Mt}{M\infty} = k_{BL} t \tag{11}$$

where k_{BL} is the release kinetic constant in Baker–Lonsdale model. The release results were fitted with the Baker–Lonsdale model. The correlation coefficient values are summarized in Table 6.

The spherical uniform shape of nanoparticles was confirmed in SEM (Fig. 1)) and AFM analysis, the mean correlation coefficient value obtained from Baker–Lonsdale model is 0.98(Table 6); which further confirms the spherical shape of nanoparticles in the release mechanism.

To confirm the structural changes occurring with nanoparticles during the simulated gastro intestinal tract study, FT-IR was performed for the nanoparticles at SGF, SDF, STIF and SCF at every 2 h interval from a wave number 1600 to 1700 cm^{-1} to predict the secondary structure modification taking place at the surface of nanoparticles during simulated conditions (Lefèvre and Subirade, 1999). FTIR spectra of β-LG nanoparticles in simulated gastro intestinal study is shown in Table 7. The spectra of β-LG nanoparticles in SGF and SDF are found to be almost similar. Spectra were similar in SGF, SDF, STIF and SCF, indicating no major modification of the β-LG structure. However some of the components located at 1624, 1635, 1648 and 1692 cm^{-1} in SGF and SDF shifted to 1623, 1634, 1647 and 1691 cm^{-1} in STIF and SCF. In SCF and STIF the intermolecular β-sheets are seen to be involved in stronger interactions thus strengthening of H-bonds between proteins.

3.6. DPPH scavenging activity of β-LG/mangiferin nanoparticles

The total antioxidant activity of mangiferin nanoparticles was 55 ± 5% of mangiferin, whereas for standard mangiferin, unencapsulated β-LG and TPP were found to be 60 ± 5%, 5 ± 2%,

Table 7
Comparison of FTIR Spectra of β-lactoglobulin nanoparticles in simulated upper gastro intestinal tract (SGF and SDF) and lower gastro intestinal tract (STIF and SCF).

Regions	Wave number (cm^{-1})	
	β-LG nanoparticles in simulated upper gastro intestinal tract	β-LG nanoparticles in simulated lower gastro intestinal tract
Regions associated with the formation of intermolecular anti-parallel β-sheets in aggregated proteins	1624 1635 1648 1678 1692	1623 1634 1647 1677 1691

2 ± 2% respectively. In a study conducted by Li et al. (2012) similar results were obtained for EGCG conjugated β-LG nanoparticles. Though the antioxidant activity encapsulated mangiferin was less in comparison with mangiferin, it could be concluded that the encapsulation protected the mangiferin from degradation and retained the antioxidant activity.

3.7. Antimicrobial activity

Nanoparticles and mangiferin (+ve control) at 400 μg/ml concentration showed antibacterial activity against *Escherichia coli* (MTCC-739)and *Staphylococcus aureus* (MTCC-441) with zones of inhibition ranging from 12 to 25 mm (Fig. 7b and Fig. 7c) and showed no sensitivity on *Bacillus subtilis* (MTCC-96) (Figs. 7a and Fig 8c), *Lactobacillus acidophilus* (MTCC-5401) (Fig. 8a), *Lactobacillus rhamnosus* (MTCC-5897) (Fig. 8b). Unencapsulated β-LG (- ve control) at 400 μg/ml showed no zone of inhibition towards the bacteria. After 24 h of incubation under aerobic condition at 37 °C, turbidity was noticed in all the test tubes of *Bacillus subtilis* (MTCC-96), *Lactobacillus acidophilus (MTCC-5401), Lactobacillus rhamnosus* (MTCC-5897) and *Escherichia coli* (JM105 K-12) containing β-LG/mangiferin nanoparticles which

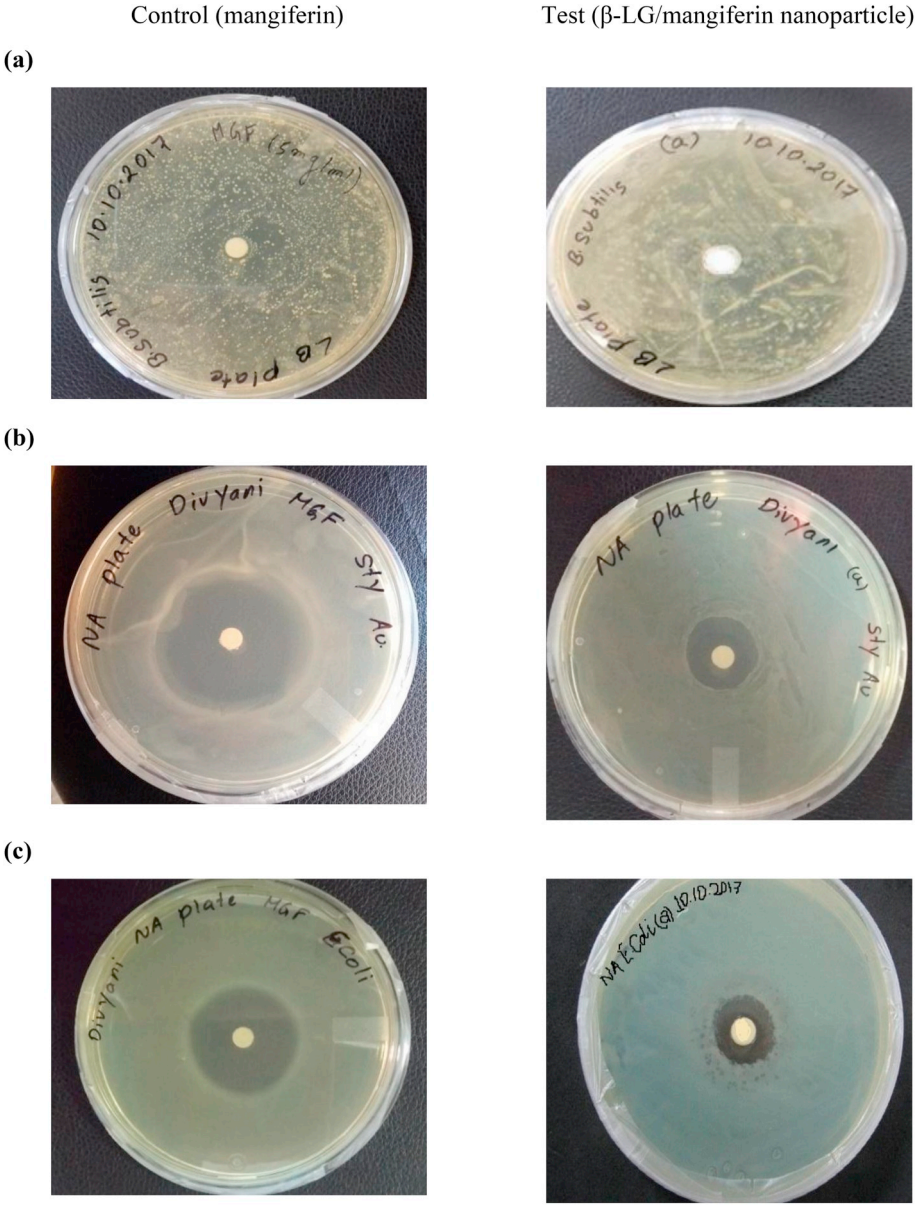

Fig. 7. Antimicrobial activity of β-LG/mangiferin(400 μg/ml) nanoparticles (a) Antimicrobial activity of Control (mangiferin 400 μg/ml) and nanoparticle against *Bacillus subtilis,* (b) Antimicrobial activity of Control (mangiferin 400 μg/ml) and nanoparticle against *Staphylococcus aureus,* (c) Antimicrobial activity of Control (mangiferin 400 μg/ml) and nanoparticle against *Escherichia coli.*

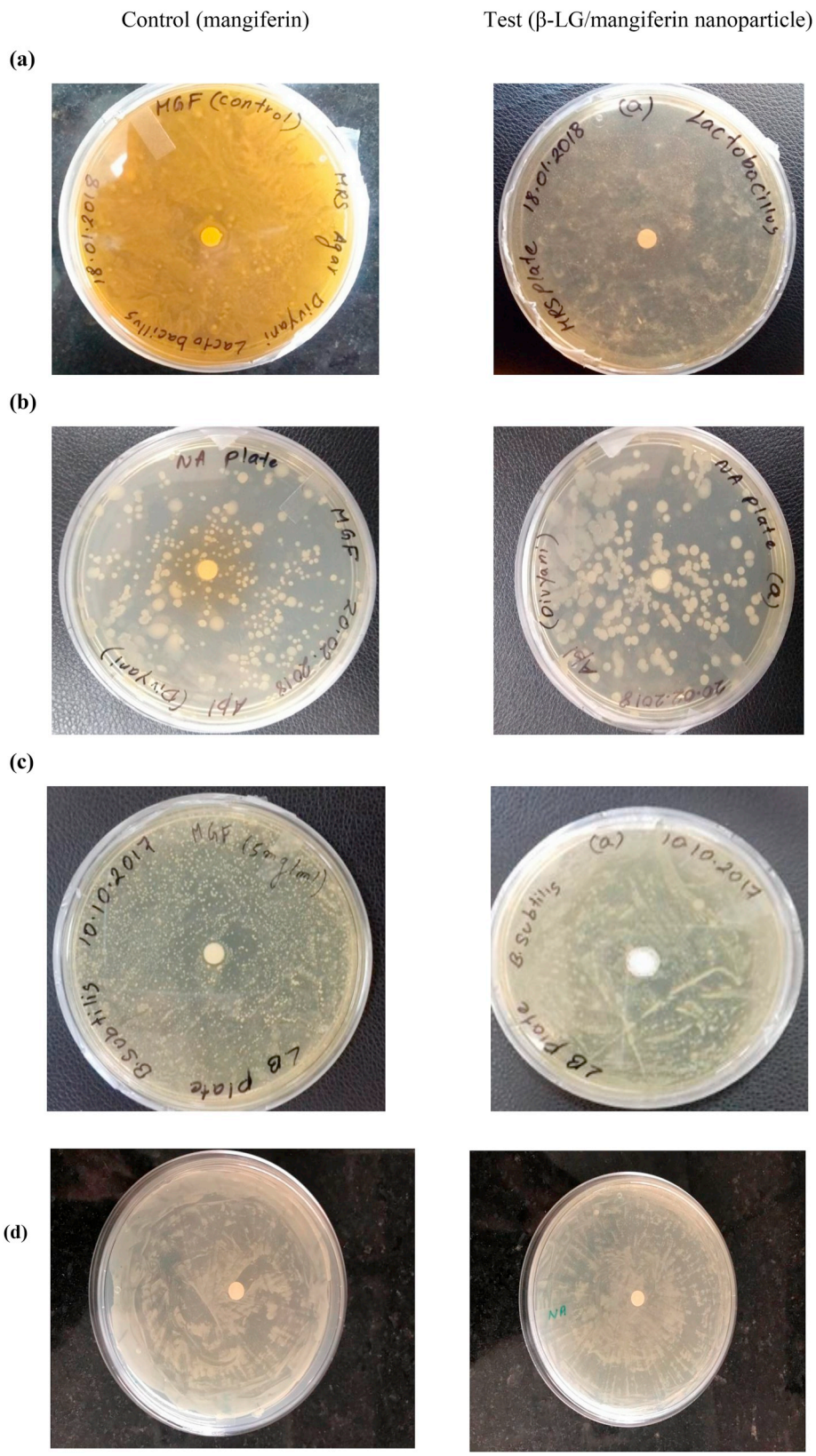

Fig. 8. Microbial Toxicity of β-lactoglobulin/mangiferin(400 μg/ml) nanoparticle (a) Microbial Toxicity of Control (mangiferin 400 μg/ml) and nanoparticles against *Lactobacillus acidophilus* (MTCC-5401), (b) Microbial Toxicity of Control (mangiferin 400 μg/ml) and nanoparticles against *Lactobacillus rhamnosus* (MTCC-5897), (c) Microbial Toxicity of Control (mangiferin 400 μg/ml) and nanoparticles against *Bacillus subtilis* (MTCC-441) and (d) Microbial Toxicity of Control (mangiferin 400 μg/ml) and nanoparticles against *Escherichia coli* (JM105 K-12).

Table 8
Bacterial growth in different concentrations of mangiferin (Control), unencapsulated β-LG nanoparticle and β-LG/mangiferin nanoparticles after 24 h.

Dilution of β-LG/mangiferin nanoparticles for the same number of bacteria in mg/ml																		
	10 mg/ml			5 mg/ml			2.5 mg/ml			1.25 mg/ml			0.625 mg/ml			0.312 mg/ml		
	M	U	B	M	U	B	M	U	B	M	U	B	M	U	B	M	U	B
E. coli (MTCC-739)	-	+	–	-	+	–	–	+	–	–	+	–	+	+	+	+	+	+
Staphylococcus aureus (MTCC-441)	-	+	–	-	-	–	–	+	–	+	+	+	+	+	+	+	+	+
Bacillus subtilis (MTCC-96)	+	+	+	+	+	+	+	+	+	+	+	+	+	+	+	+	+	+
Lactobacillus acidophilus (MTCC-5401)	+	+	+	+	+	+	+	+	+	+	+	+	+	+	+	+	+	+
Lactobacillus rhamnosus (MTCC-5897)	+	+	+	+	+	+	+	+	+	+	+	+	+	+	+	+	+	+
Escherichia coli (JM105 K-12)	+	+	+	+	+	+	+	+	+	+	+	+	+	+	+	+	+	+

M: Mangiferin (control).
U: unencapsulated β-LG nanoprticle
B: β-LG/mangiferin nanoparticles.
Positive (+) = Turbidity indicating growth.
Negative (−) = No turbidity indicating absence of growth.

Table 9
Minimum Bactericidal Concentrations of mangiferin (control), unencapsulated β-LG (control) nanoparticle and β-LG/mangiferin nanoparticles after 24 h.

	Dilution of mangiferin (control)		Dilution of unencapsulated β-LG nanoparticles (control)		Dilution of β-LG/mangiferin nanoparticles	
E. coli (MTCC-739)	-	-	+	+	–	–
Staphylococcus aureus (MTCC-441)	-	-	+	+	–	–
Bacillus subtilis (MTCC-96)	+	+	+	+	+	+
Lactobacillus acidophilus (MTCC-5401)	+	+	+	+	+	+
Lactobacillus rhamnosus (MTCC-5897)	+	+	+	+	+	+
Escherichia coli (JM105 K-12)	+	+	+	+	+	+

Positive (+) = Indicating growth.
Negative (−) = Indicating absence of growth.

indicated that nanoparticles doesnot have toxicity towards the useful probiotic strains (Tables 8 and 9), while towards *E. coli* (MTCC-739) and *Staphylococcus aureus* (MTCC-441) at a concentration of 1.25 mg/ml *and* 2.5 mg/ml of nanoparticle concentration inhibited the growth of bacteria (Table 8), hence confirming the bactericidal effect of the nanoparticle (Table 8). These results thus confirms that the MIC and MBC of β-LG/mangiferin nanoparticles against was found to be effective *Escherichia coli* (MTCC-739) at 1.25 mg/ml and *Staphylococcus aureus* (MTCC-441) at 2.5 mg/ml. Controls in the present study were mangiferin and unencapsulated β-LG nanoparticles at a concentration range from 0.312 to 10 mg/ml (Table 8).

3.8. Microbial toxicity

Microbial toxicity study showed that the nanoparticles do not show toxicity towards the strains of the gut (Fig. 8) (Tables 8 and 9) Hence the oral consumption of the nanoparticles would not inhibit the useful strains in the gut like *Lactobacillus acidophilus* (MTCC- 5401), *Bacillus subtilis* (MTCC-441), *Lactobacillus rhamnosus* (MTCC-5897) and *Escherichia coli* (JM105 K-12).

4. Conclusions

To answer the problems associated with the low systemic availability and diminished efficacy of mangiferin during oral administration, nanoencapsulation technique was used with β-LG protein. The prepared nanoparticle had a size of 89 ± 10 nm and a zeta potential of −30.0 ± 0.2 mV and an encapsulation efficiency of 85%. AFM and SEM analysis exhibited the uniform size and shape of nanoparticles which was further assured by the mean correlation coefficient value obtained from Baker–Lonsdale model. The *in vitro* release mechanism showed the controlled release of mangiferin under simulated GI condition. Maximum release of 80% occurred at 8hr in the colon fluid. The FTIR study confirmed that mangiferin was successfully encapsulated in β-LG. B-LG/mangiferin nanoparticle was stable at 4 °C for 30 days. Nanoencapsulation protected mangiferin from degradation as well as retained the antioxidant activity. This study also showed that nanoparticle had an inhibition on the growth of various gram-negative microorganisms significantly. Nanoparticles have shown protection towards the probiotic strains in a GI tract. It can be foreseen that nanoparticle can be effectively utilised in pharmaceutical and nutraceutical industries for their high antimicrobial and antioxidant activities. It is concluded that β-LG nanoparticle containing mangiferin may be a promising candidate for the oral delivery of site-directed target in future.

Acknowledgment

We thank CSIR - Central Mechanical Engineering Research Institute, Durgapur, West Bengal, India for the technical support they have extended for this work.

Appendix A. Supplementary data

Supplementary data related to this article can be found at https://doi.org/10.1016/j.jfoodeng.2018.11.020.

References

Ahuja, N., Katare, O.P., Singh, B., 2007. Studies on dissolution enhancement and mathematical modeling of drug release of a poorly water-soluble drug using water-soluble carriers. Eur. J. Pharm. Biopharm. 65, 26–38. https://doi.org/10.1016/j.ejpb.2006.07.007.

Andriani, Y., Grastianto, Siswanta, Mudasir, 2015. Glutaraldehyde-crosslinked chitosan-pectin nanoparticles as a potential Carrier for curcumin delivery and its in vitro release study. Int. J. Drug Deliv. 7, 167–173.

Balouiri, M., Sadiki, M., Ibnsouda, S.K., 2016. Methods for in vitro evaluating antimicrobial activity : a review $. J. Pharm. Anal. 6, 71–79. https://doi.org/10.1016/j.jpha.2015.11.005.

Chandra, D., 2017. Phytochemical and ethnomedicinal uses of family gentianaceae. Curr. Res. Chem. 8, 1–9. https://doi.org/10.3923/crc.2016.1.9.

Chen, L., Remondetto, E., Subirade, M., 2006. Food protein-based materials as nutraceutical delivery systems. Trends Food Sci. Technol. 17, 272–283. https://doi.org/10.1016/j.tifs.2005.12.011.

Ghalandari, B., Divsalar, A., Akbar, A., Parivar, K., 2014. Journal of Photochemistry and Photobiology B : biology the new insight into oral drug delivery system based on metal drugs in colon cancer therapy through b -lactoglobulin/oxali-palladium nanocapsules. J. Photochem. Photobiol. B Biol. 140, 255–265. https://doi.org/10.1016/j.jphotobiol.2014.08.003.

Gibbs, B.F., Kermasha, S., Alli, I., Mulligan, C.N., 1999. Encapsulation in the food industry : a review. Int. J. Food Sci. Nutr. 50, 213–224.

Gonza, A.F., 2007. Effect of β -lactoglobulin A and B whey protein variants on the rennet-induced gelation of skim milk gels in a model reconstituted skim milk system. J. Dairy Sci. 90, 582–593. https://doi.org/10.3168/jds.S0022-0302(07)71541-2.

Haug, I.J., Skar, H.M., Vegarud, G.E., Langsrud, T., Draget, K.I., 2009. Electrostatic effects on b -lactoglobulin transitions during heat denaturation as studied by differential scanning calorimetry. Food Hydrocolloids 23, 2287–2293. https://doi.org/10.1016/j.foodhyd.2009.06.006.

Higuchi, T., 1963. Mechanism of sustained- action medication theoretical analysis of rate of release of solid drugs dispersed in solid matrices. J. Pharmacol. Sci. 52, 1145–1149.

Hixson, A., Crowell, J., 1931. Dependence of reaction velocity upon surface and agitation. Ind. Eng. Chem. 23, 923–931.

Hurkat, P., Jain, A., Jain, A., 2012. Concanavalin A conjugated biodegradable nanoparticles for oral insulin delivery. J. Nanoparticle Res. 14. https://doi.org/10.1007/s11051-012-1219-4.

Jahanshahi, M., Babaei, Z., 2008. Protein Nanoparticle : a Unique System as Drug Delivery Vehicles, vol. 7. pp. 4926–4934.

Jones, O.G., Handschin, S., Adamcik, J., Harnau, L., Bolisetty, S., 2011. Complexation of β -lactoglobulin fibrils and sulfated polysaccharides. Biomacromolecules 12, 3056–3065. https://doi.org/10.1021/bm200686r.

Joubert, E., 2012. Rapid screening methods for estimation of mangiferin and xanthone contents of Cyclopia subternata plant material. South Afr. J. Bot. 82, 113–122. https://doi.org/10.1016/j.sajb.2012.07.019.

Karim, A.A., Azlan, A., 2012. Fruit pod extracts as a source of nutraceuticals and pharmaceuticals. Molecules 17, 11931–11946. https://doi.org/10.3390/molecules171011931.

Kawakami, C.M., Gaspar, L.R., 2015. Mangiferin and naringenin affect the photostability and phototoxicity of sunscreens containing avobenzone. J. Photochem. Photobiol. B Biol. 151, 239–247. https://doi.org/10.1016/j.jphotobiol.2015.08.014.

Ko, S., Gunasekaran, S., 2006. Preparation of sub-100-nm b -lactoglobulin (BLG) nanoparticles. J. Microencapsul. 23, 887–898. https://doi.org/10.1080/02652040601035143.

Korsmeyer, R.W., Gumy, R., Doelker, E., Buri, P., Peppas, N.A., 1983. Mechanisms of solute release from porous hydrophilic polymers. Int. J. Pharm. 15, 25–35.

Kosmidis, K., Argyrakis, P., 2003. A reappraisal of drug release laws using Monte Carlo Simulations : the prevalence of the Weibull function. Pharm. Res. (N. Y.) 20, 988–995.

Krishnan, R., Arumugam, V., Vasaviah, S.K., 2015. The MIC and MBC of silver nanoparticles against Enterococcus faecalis - a facultative anaerobe. J. Nanomed. Nanotechnol. 06. https://doi.org/10.4172/2157-7439.1000285.

Kullu, J., Dutta, A., Constales, D., Chaudhuri, S., Dutta, D., 2014. Experimental and modeling studies on microwave-assisted extraction of mangiferin from Curcuma amada. 3 Biotech 4, 107–120. https://doi.org/10.1007/s13205-013-0125-5.

Larsson, M., Hill, A., Duffy, J., 2012. Suspension Stability ; why particle size , zeta potential and rheology are important. Annu. Trans. Nord. Rheol. Soc. 20, 209–214.

Lefèvre, T., Subirade, M., 1999. Structural and interaction properties of β-lactoglobulin as studied by FTIR spectroscopy. Int. J. Food Sci. Technol. 34, 419–428. https://doi.org/10.1046/j.1365-2621.1999.00311.x.

Li, B., Du, W., Jin, J., Du, Q., 2012. Preservation of (-)-epigallocatechin-3-gallate antioxidant properties loaded in heat treated β-lactoglobulin nanoparticles. J. Agric. Food Chem. 60, 3477–3484. https://doi.org/10.1021/jf300307t.

Liang, J., Yan, H., Wang, X., Zhou, Y., Gao, X., Puligundla, P., Wan, X., 2017. Encapsulation of epigallocatechin gallate in zein/chitosan nanoparticles for controlled applications in food systems. Food Chem. 231, 19–24. https://doi.org/10.1016/j.foodchem.2017.02.106.

Lobo, M.S., Costa, P., 2001. Modeling and comparison of dissolution profiles ´. Eur. J. Pharmaceut. Sci. 13, 123–133.

Luo, Y., Teng, Z., Wang, Q., 2012. Development of zein nanoparticles coated with carboxymethyl chitosan for encapsulation and controlled release of vitamin D3. J. Agric. Food Chem. 60, 836–843. https://doi.org/10.1021/jf204194z.

Luo, Y., Zhang, B., Whent, M., Yu, L.L., Wang, Q., 2011. Colloids and Surfaces B : biointerfaces Preparation and characterization of zein/chitosan complex for encapsulation of ˛ -tocopherol , and its in vitro controlled release study. Colloids Surfaces B Biointerfaces 85, 145–152. https://doi.org/10.1016/j.colsurfb.2011.02.020.

M02-A12: Performance Standards for Antimicrobial Disk Susceptibility Tests; Approved Standard—Twelfth Edition, 2015.

Malsuno, R., Adachi, S., 1993. Lipid encapsulation technology- techniques and applications to food. Trends Food Sci. Technol. 4, 781–785.

Mcconnell, E.L., Fadda, H.M., Basit, A.W., 2008. Gut instincts : explorations in intestinal physiology and drug delivery. Int. J. Food Sci. Nutr. 364, 213–226. https://doi.org/10.1016/j.ijpharm.2008.05.012.

Nijs, A., Cartuyvels, R., Mewis, A., Peeters, V., Rummens, J.L., Magerman, K., 2003. Comparison and evaluation of osiris and sirscan 2000 antimicrobial susceptibility systems in the clinical microbiology laboratory. J. Clin. Microbiol. 41, 3627–3630. https://doi.org/10.1128/JCM.41.8.3627.

Rao, J., Mcclements, D.J., 2011. formation of flavor oil microemulsions , nanoemulsions and Emulsions : influence of composition and preparation method. J. Agric. Food Chem. 59, 5026–5035. https://doi.org/10.1021/jf200094m.

Relkin, P., 1998. Reversibility of heat-induced conformational changes and surface exposed hydrophobic clusters of β-lactoglobulin: their role in heat-induced sol-gel state transition. Int. J. Biol. Macromol. 22, 59–66. https://doi.org/10.1016/S0141-8130(97)00089-5.

Saadati, Z., Razzaghi, A., 2012. Comparative analysis of chemical and thermal denatured β -lactoglobulin AB in the presence of casein. Adv. Stud. Biol. 4, 255–264.

Saha, S., Roy, A., Roy, K., Roy, M.N., 2016. Study to explore the mechanism to form inclusion complexes of β -cyclodextrin with vitamin molecules. Nat. Publ. Gr. 1–12. https://doi.org/10.1038/srep35764.

Sakurai, K., Oobatake, M., 2001. Salt-dependent monomer – dimer equilibrium of bovine ˛ -lactoglobulin at pH 3. Protein Sci. 10, 2325–2335. https://doi.org/10.1101/ps.17001.milk.

Sari, T.P., Mann, B., Kumar, R., Singh, R.R.B., Sharma, R., Bhardwaj, M., Athira, S., 2015. Preparation and characterization of nanoemulsion encapsulating curcumin. Food Hydrocolloids 43, 540–546. https://doi.org/10.1016/j.foodhyd.2014.07.011.

Souza, S.D., 2014. A review of in vitro drug release test methods for nano-sized dosage forms. Adv. Pharm. 2014, 1–12. https://doi.org/10.1155/2014/304757.

Stoica, R., Ion, R.M., 2013. Preparation of chitosan tripolyphosphate nanoparticles for the encapsulation of polyphenols extracted from rose hips. Dig. J. Nanomater. Biostructures 8, 955–963.

Teng, Z., Luo, Y., Li, Y., Wang, Q., 2016. Cationic beta lactoglobulin nanoparticles as a bioavailability enhancer: effect of surface properties and size on the transport and delivery in vitro. Food Chem. 391–399. https://doi.org/10.1016/j.foodchem.2016.02.139.

Teng, Z., Xu, R., Wang, Q., 2015. Beta-lactoglobulin-based encapsulating systems as emerging bioavailability enhancers for nutraceuticals: a review. RSC Adv. 5, 35138–35154. https://doi.org/10.1039/c5ra01814e.

Zhao, C., Shen, X., Guo, M., 2018. Stability of lutein encapsulated whey protein nanoemulsion during storage. PLoS One 13, 1–10. https://doi.org/10.1371/journal.pone.0192511.

Zuidam, N.J., Shimoni, E., 2010. Overview of Microencapsulates for Use in Food Products or Processes and Methods to Make Them 3–30.